한국정밀공학회지 제16권 제 4호 (1999년 4월)
Journal of the Korean Society of Precision Engineering Vol. 16, No. 4, April 1999.

빠른 하중을 받고 있는 3점 굽힘 시험편들의 다양한 동적거동

이억섭*, 조재웅**, 한문식***

Various Dynamic Behavior of Three Point Bend Specimens under Rapid Loading

Ouk Sub Lee*, Jae Ung Cho**, and Moon Sik Han***

ABSTRACT

충격하중을 받는 시험편 높이의 1/4 길이의 notch를 가진 3점 굽힘시험편들의 기계적 거동에 관한 컴퓨터 시뮬레이션을 하고 이 시뮬레이션에 대한 실험적 검증도 하여 그 타당성을 입증하였다. 시험편들의 양쪽 가장자리(지지점)에서 작용되어지는 여러 가지의 하중속도에 대한 경우들과 탄소성 von Mises 재질인 모델들을 시뮬레이션에 포함시켰으며 이들에 대한 결과들을 간극 개구 변위, 반력, 크랙선단 개구 변위 및 변형률등이 속도에 의존되는 재질(점소성 재질)에 대한 시뮬레이션 결과와 비교하였다. 또한 여러 가지의 동적 하중을 받는 상황하에서의 안정성이 본 연구의 시뮬레이션을 통하여 비교되었으며 그 차이점들이 규명되었다.

Key Words : Dynamic Fracture(동적파괴), Gap Opening Displacement(간극개구 변위), Crack Tip Opening Displacement(크랙선단개구변위), Strain Rate(변형률속도), Visco-plastic Material(점소성재료)

1. Introduction

In experiments and analyses of dynamic fracture, three point bend specimens are popularly used as in the finite element analyses by Kalthoff[1], Kanninen[2], Rosakis[3], Van Elst[4], and Ahmad[5].

Most experiments have been performed by using the drop weight which applies a load to the middle point(position) of a specimen(Point A in Fig.2).

However, loading rates are somewhat limited in many published experiments. Therefore, high speed track with high performance[6] is used to investigate dynamic fracture behavior of structure under high loading rate. The high speed track used by Wihlborg[6] can produce impact speeds in the range of 10m/s to 60m/s.

* 정회원, 인하대학교
** 정회원, 천안공업대학 자동차과
*** 정회원, 계명대학교 자동차공학부

In this paper, computer simulations are investigate the dynamic behavior of popularly used three-bend specimens under various loading rates. The simulations include plasticity and visco-plasticity behavior of the specimen material. The stability in dynamic fracture of the material is also considered.

2. Finite Element Model

We make numerical simulation by using ABAQUS, commercial FEM code[7]. An elastoplastic von Mises model is assumed for mild steel specimens used in this research which have following physical properties:

Young's Modulus(E) = 206 GPa,

Poisson's Ratio(ν) = 0.3,

Density(ρ) = 7800 Kg/m^3

Yielding stress(σ_Y) = 360 MPa

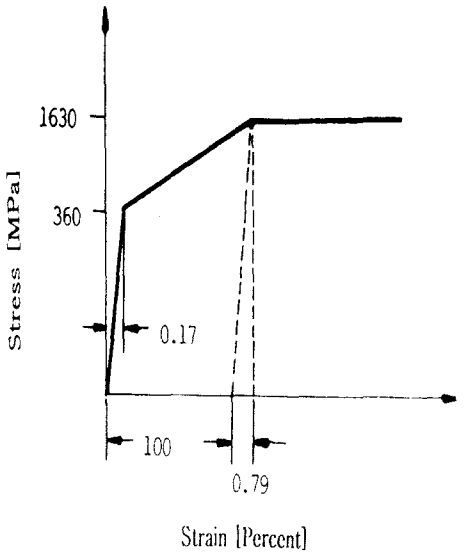

Fig. 1 Static stress-strain curve of the material of a three-point specimen used in our research

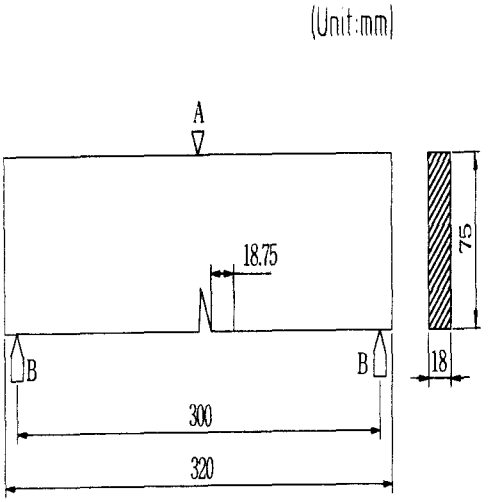

Fig. 2 Three point bend specimen with a quarter notch

The brittleness and ductility are clearly shown at the fracture surface of the thick specimen applied to high impact velocity[8]. The influence of thickness is rarely shown at the fracture surface of the thin specimen applied to high impact velocity. Therefore, the thickness of specimen can be determined as thin as 18 mm. Fig.2 shows the shape of the specimen which has a crack which size is a quarter of its height. Half of the specimen is considered in the computer simulation because of its geometric symmetry. We choose a two-dimensional finite element model with 92 of 8 node points in our simulation as shown in Fig. 3. Furthermore, one side of eight node point elements near a crack tip concentrates on the crack tip. The impact in dynamic fracture experiment [9] causes a specimen to rebound in the air by very small amount. The rebound makes a gap between load and support points which is called gap opening displacement. We compute the gap opening displacement and reaction forces on gap elements and the results are shown in Fig. 3.

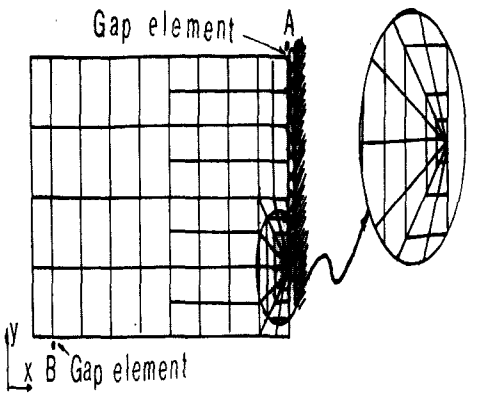

Fig. 3 The finite element model

3. Boundary Conditions, Visco-Plasticity and Inspection of Specimen Model

Dynamic load is applied to the imaginary point B on the model as shown in Fig. 3.

The dynamic load is 1.96kN and the impact-starting time at the impact head is considered to be 'zero'. Impact speeds(V) are taken as 15, 30, 45 and 60m/s. The impact speed is assumed to remain constant after being applied at '0' time.

Simulation is performed for the period from '0' to 600 μs over which crack does not propagate. In this simulation, we assume the velocity-dependent material characteristic used in Malvern visco-elastic model, one-dimensional from[10] of which is

$$\dot{\varepsilon}^{vp} = \beta\left(\frac{\sigma}{\sigma_Y} - 1\right)^n$$

Here, $\dot{\varepsilon}^{vp}$ is plastic strain, σ stress, and σ_Y yielding stress. β and n are visco-plastic coefficients which are chosen to be 4000 and 2, respectively[11].

The experimental display is also shown in Fig.4.

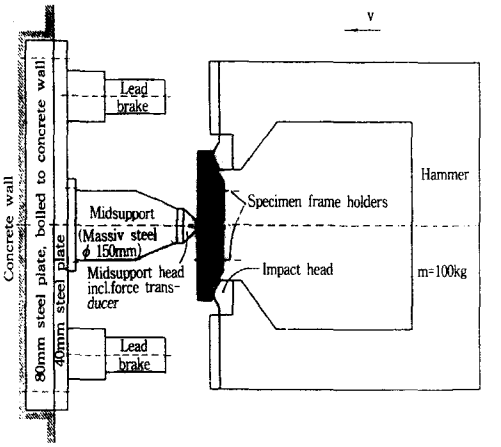

Fig. 4 Cited experimental display

The U-shaped hammer is accelerated to a prescribed velocity and hits the 3PB specimen at its ends. Two hardened and tempered impact heads with cylindrical contact surfaces are attached to the hammer. The experiments of cited paper[8] were carried with impact velocities of 30 m/s and 45 m/s. The dimensions of designed specimen in this experiment are shown in Fig.5.

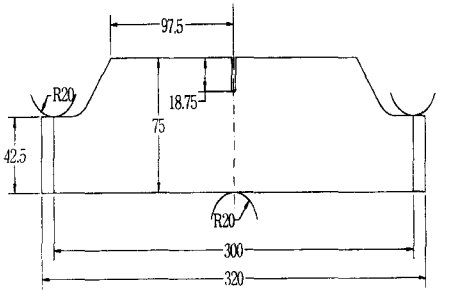

Fig. 5 Dimensions of the new designed 3PB specimens of cited experiment (All dimensions are in mm.)

The mid-support forces for the simulations together with the experimental result are shown with impact velocities of 30 m/sec and 45 m/sec, respectively in Fig. 6 and Fig.7.

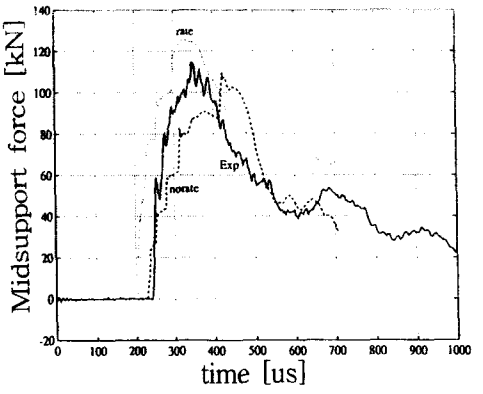

Fig. 6 Mid-support force versus time at 30m/s impact velocity for the two different simulations and the experiment (experiment:full line, simulations, no rate: broken line, rate:dotted line)

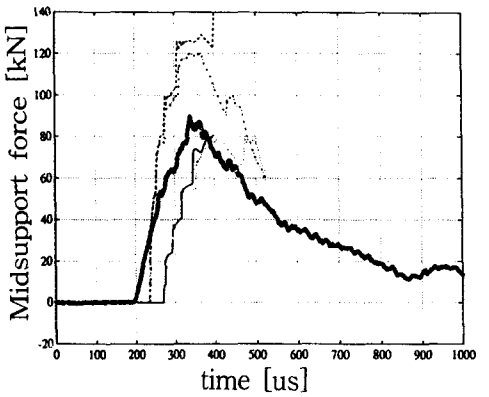

Fig. 7 Mid-support force versus time at 45m/s impact velocity for the four different simulations and the experiment (experiment:thick line, simulations, no rate and no crack growth:dotted line, rate and no crack growth:broken line, rate and crack growth:point line)

The simulation including viscoplastic properties is more close to the experimental result. The simulations are combinations of with and without rate influence and with and without crack growth. They are denoted as rate-no rate and crack growth-no crack growth. Good agreement between the experiments and the numerical simulations was obtained for the case of 30 m/sec impact loading. The CTODs as function of time are also shown with impact velocities of 30 m/sec in Fig. 8.

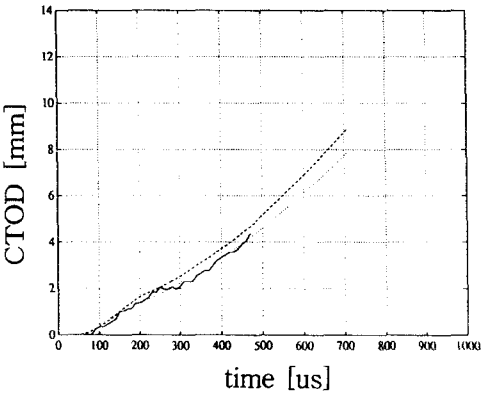

Fig. 8 CTOD at 30m/s impact velocity for the two different simulations and the experiment (experiment:full line, simulations, no rate: broken line, rate:dotted line)

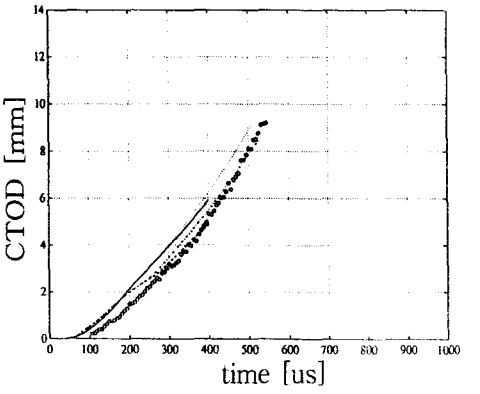

Fig. 9 CTOD at 45m/s impact velocity for the four different simulations and the experiment (experiment:circles, simulations, no rate and no crack growth:dotted line, rate and no crack growth:broken line, rate and crack growth:point line)

As is seen from the figure, the experimental CTOD is close to the simulation including the rate influence. Fig. 9 shows CTOD as a function of time with the impact velocity of 45 m/sec. The best fit by the simulation to the experiment is obtained when viscoplastic and crack propagation properties ate included. Therefore, the inspection of this specimen model in this presented paper is sufficient for numerical simulation.

4. Simulation Results for Dynamic Behavior

Computed gap opening displacements and reaction forces for visco-plastic material are compared with those for non-visco-plastic material. We also investigate the change of crack tip opening displacement (CTOD) and strain rate with time under the various dynamic loadings.

4.1 Reaction Forces and Gap Opening Displacements

Figs. 10～13 show the change of reaction forces at loading point A and supporting point B and Gap Opening Displacement at A for non-visco-plastic specimens with respect to time variation.

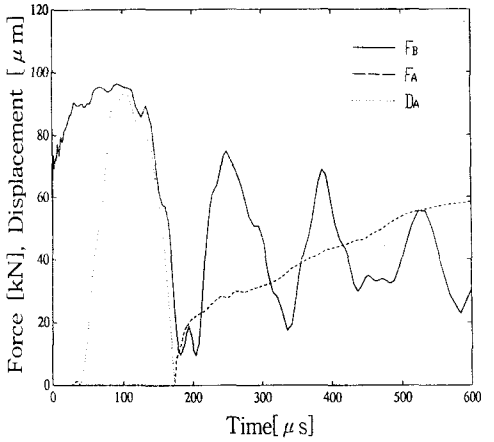

Fig. 10 Dynamic responce by impact at the side point B; V_B=15m/s(no visco-plasticity)
F_B=Reaction force at B
F_A=Reaction force at A
D_A=Gap opening displacement at A

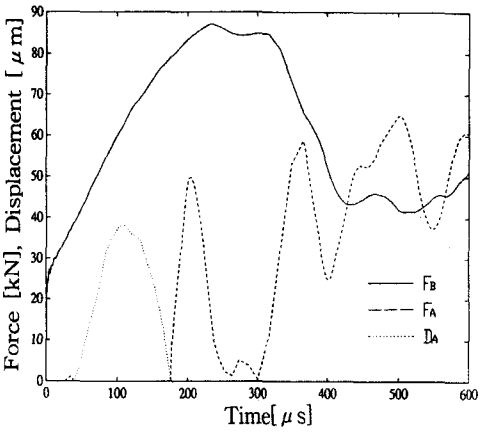

Fig. 11 Dynamic responce by impact at the side point B; V_B=30m/s(no visco-plasticity)
F_B=Reaction force at B
F_A=Reaction force at A
D_A=Gap opening displacement at A

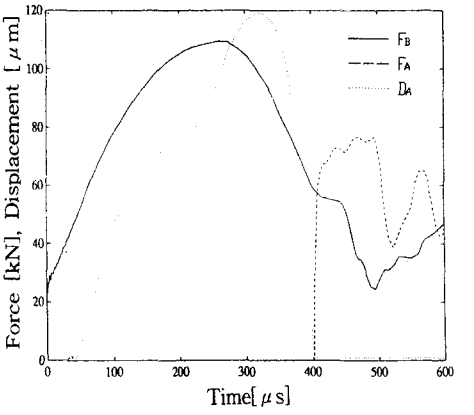

Fig. 12 Dynamic responce by impact at the side point B; V_B=45m/s(no visco-plasticity)
F_B=Reaction force at B
F_A=Reaction force at A
D_A=Gap opening displacement at A

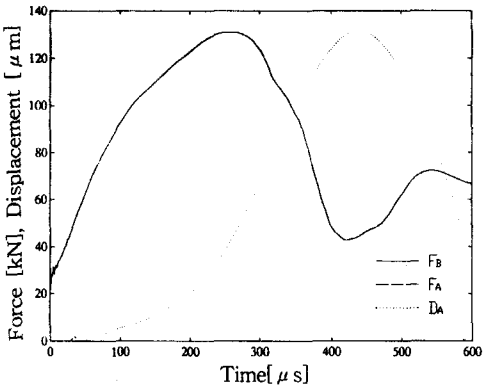

Fig. 13 Dynamic responce by impact at the side point B; V_B=60m/s(no visco-plasticity)
F_B=Reaction force at B
F_A=Reaction force at A
D_A=Gap opening displacement at A

F_B is the reaction force at point B and F_A is half the reaction force at point A. Loading rate for Fig. 10 is 15m/s. F_B is suddenly raised to 70kN shortly after impact and increases up to 100kN. Stress wave reaches at the point A 28 μs after impact and induces a small-magnitude reaction force F_A at the point A. The reaction force F_A holds for about 10 μs after which the specimen separates from the contact at the point A. Maximum gap opening displacement D_A becomes 0.094mm about 103 μs later. The gap at point A is closed again 170 μs after impact. F_A is rapidly increased to 20kN, and then increases linearly. F_B vibrates by damping with a period of 150 μs and the vibrating period decreases slightly with time.

Loading rate in Fig.11 is 30m/s. Maximum reaction force F_B becomes less than 90kN, and F_B fluctuates after it becomes about 50kN. Maximum gap opening displacement D_A opens a little wider to become about 40 μm.

Fig. 12 shows the results for the case of loading rate of 45m/s for which maximum reaction force F_B becomes larger than 100kN and F_A drops to less than 80kN. Maximum gap opening displacement D_A widens to 120 μm.

In Fig. 13 where loading rate is 60m/s. F_B rises to about 130kN. Maximum gap opening displacement D_A increases to 130 μm, and reaction force F_A does not occur until 600 μs after impact.

Figs. 14~17 show reaction forces and gap opening displacement with time for visco-plastic specimens.

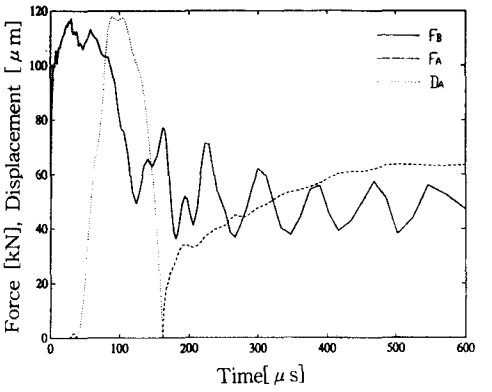

Fig. 14 Dynamic responce by impact at the side point B; V_B=15m/s(visco-plasticity)
F_B=Reaction force at B
F_A=Reaction force at A
D_A=Gap opening displacement at A

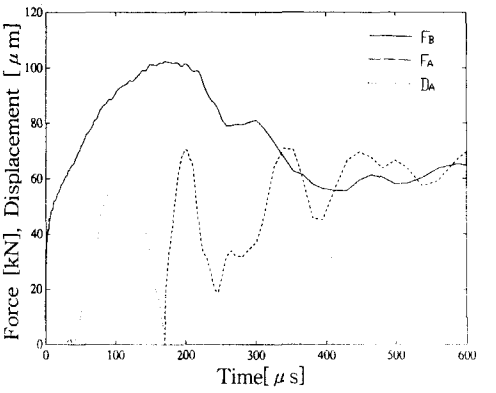

Fig. 15 Dynamic responce by impact at the side point B; V_B=30m/s(visco-plasticity)
F_B=Reaction force at B
F_A=Reaction force at A
D_A=Gap opening displacement at A

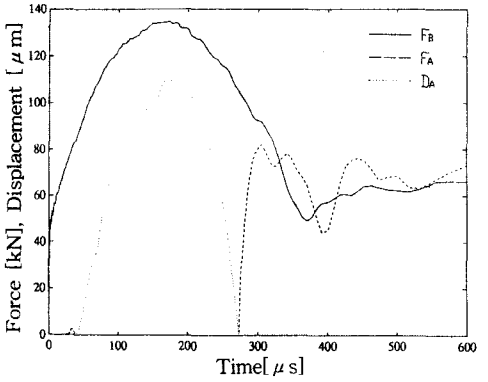

Fig. 16 Dynamic responce by impact at the side point B; V_B=45m/s(visco-plasticity)
F_B=Reaction force at B
F_A=Reaction force at A
D_A=Gap opening displacement at A

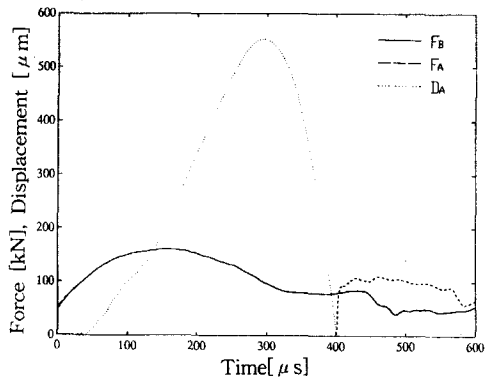

Fig. 17 Dynamic responce by impact at the side point B; V_B=60m/s(visco-plasticity)
F_B=Reaction force at B
F_A=Reaction force at A
D_A=Gap opening displacement at A

Fig. 14 is the case of loading rate 15m/s for which maximum values of F_B, D_A, and F_A are 120kN, 120 μm, and 60kN, respectively. In Fig. 15 with loading rate 30m/s, F_B and D_A have maximum values of 100kN and 60 μm, respectively, and F_A fluctuates after it reaches the value of 70kN. The loading rate in Fig. 16 is 45m/s for which F_B and D_A have maximum values of 135kN and 110 μm, respectively. Reaction force F_A fluctuates after it reaches a value of 80kN. In case of a loading rate of 60m/s as shown in Fig. 17, maximum values of F_B, D_A, and F_A are 150kN, 550 μm, and 100kN, respectively.

4.2 Strain rates and CTODs

Figs. 18~21 show $\dot{\varepsilon}_{xx}$(strain rate in the x direction) with time of non-visco plastic specimens at positions near the crack tip.

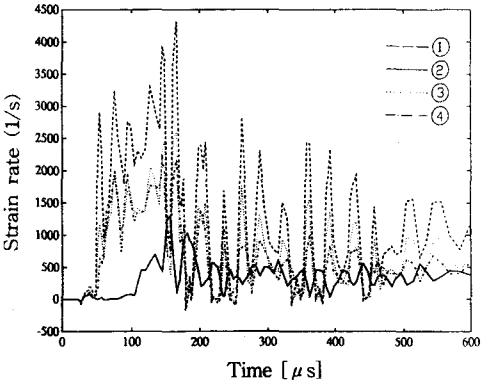

Fig. 18 Strain rate according to time at 1,2,3,4 positions; V_B=15m/s(no visco-plasticity)

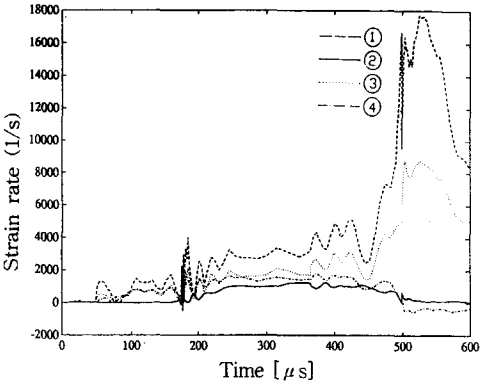

Fig. 19 Strain rate according to time at 1,2,3,4 positions; V_B=30m/s(no visco-plasticity)

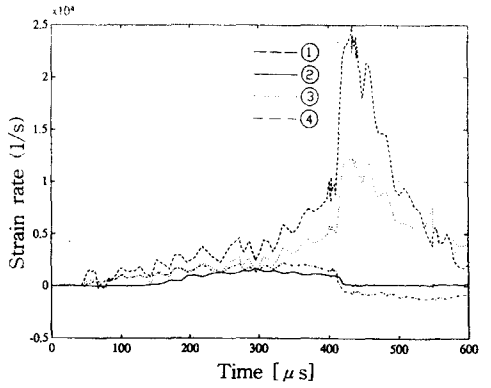

Fig. 20 Strain rate according to time at 1,2,3,4 positions; V_B=45m/s(no visco-plasticity)

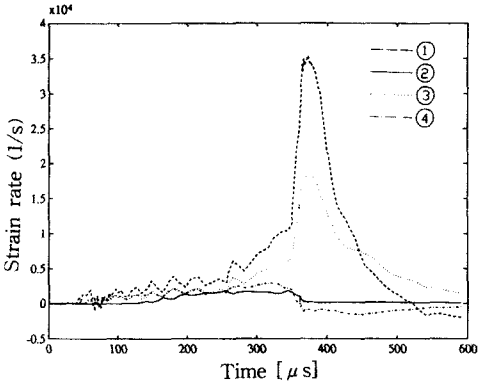

Fig. 21 Strain rate according to time at 1,2,3,4 positions; V_B=60m/s(no visco-plasticity)

Loading rates for Figs. 18~21 are 15,30,45, and 60m/s, respectively. The positions at the crack tip are denoted by ①, ②, ③, and ④ as in Fig.22.

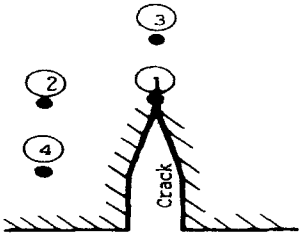

Fig. 22 The positions near crack tip

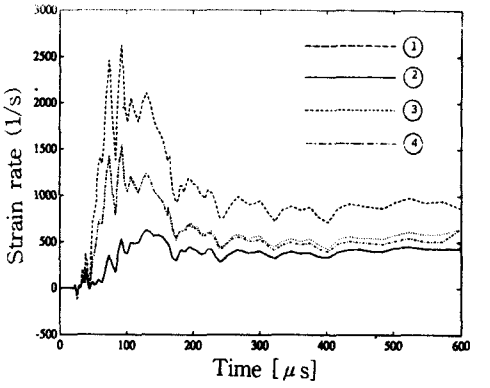

Fig. 23 Strain rate according to time at 1,2,3,4 positions; V_B=15m/s(visco-plasticity)

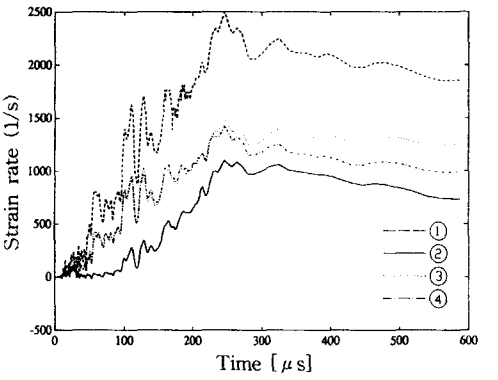

Fig. 24 Strain rate according to time at 1,2,3,4 positions; V_B=30m/s(visco-plasticity)

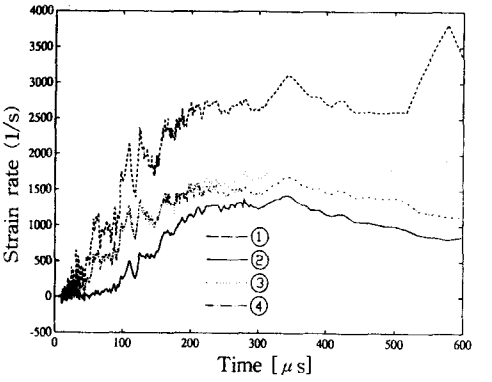

Fig. 25 Strain rate according to time at 1,2,3,4 positions; V_B=45m/s(visco-plasticity)

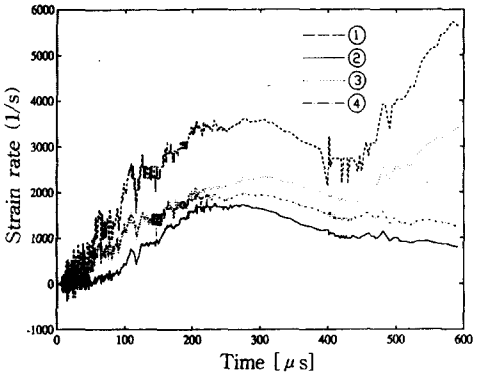

Fig. 26 Strain rate according to time at 1,2,3,4 positions; V_B=60m/s(visco-plasticity)

In Figs. 18~21 and Figs. 23~26 dashed lines(---), solid lines(——), dotted lines(···), and dot-dashed lines(- · - · -) represent strain rates at the positions ①, ②, ③, and ④, respectively. We can notice that $\dot{\varepsilon}_{xx}$ at the position ① has the largest value and determines the fracture by dynamic crack. The strain rate $\dot{\varepsilon}_{xx}$ is 4300/s at about 150 μs with 15m/s in Fig.18, and 1800/s at about 550 μs with 30m/s in Fig.19. In Fig. 20 with 45m/s $\dot{\varepsilon}_{xx}$ becomes 25000/s at about 400 μs, and in Fig.21 with 60m/s $\dot{\varepsilon}_{xx}$ reaches 35000/s at about 370 μs. Figs. 23~26 show $\dot{\varepsilon}_{xx}$ with time of visco-plastic specimens at positions near a crack tip when loading rates are 15m/s, 30m/s, 45m/s, and 60m/s, respectively. The same maximum strain rates($\dot{\varepsilon}_{xx}$) of 2800/s occur at 100 μs and 250 μs in Fig.23 with 15m/s and Fig.24 with 30m/s, respectively. The maximum strain rates in case of 45m/s in Fig.25 and 60m/s in Fig.26 occur at about the same time of 570 μs. The maximum $\dot{\varepsilon}_{xx}$ is 3800/s for 45m/s and 5700/s for 60m/s.

Figs. 27 and 28 are cack tip opening displacement(CTOD) curves with time for non-visco plastic specimens and visco-plastic specimens, respectively with loading rates of 15, 30, 45, and 60m/s.

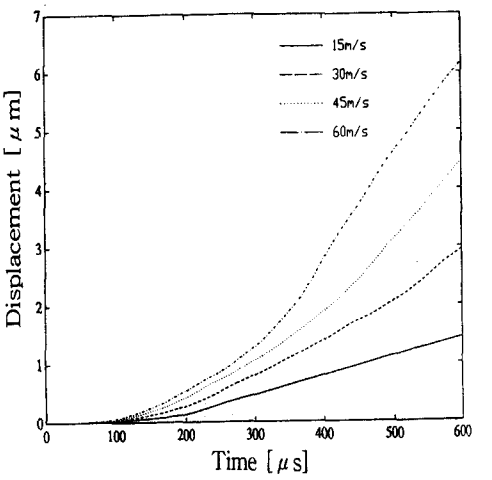

Fig. 27 Crack tip opening displacement according to time at various loading rates; V_B=15,30,45,60m/s(no visco-plasticity)

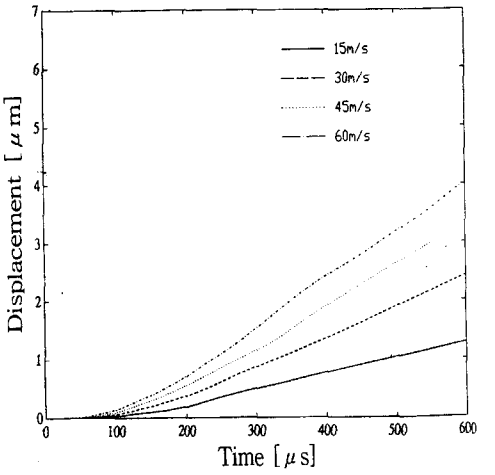

Fig. 28 Crack tip opening displacement according to time at various loading rates; V_B=15,30,45,60m/s(visco-plasticity)

Fig. 29 shows the simulation of the midsupport force as a function of time for the 30 m/s impact velocity case. The notations (rate and norate) indicate the result from simulations with and without rate depending material properties.

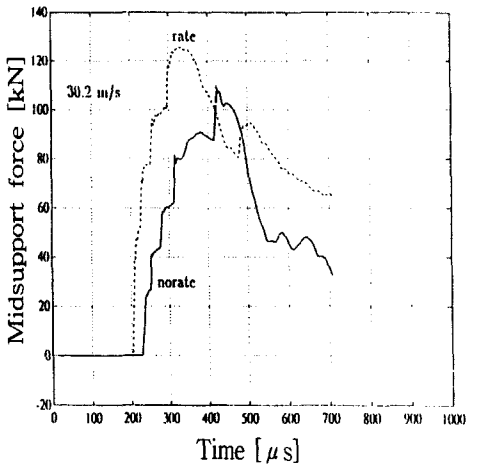

Fig. 29 Influence of the viscoplastic material properties on the midsupport force for 30m/s impact velocity case

5. Considerations

As shown in Figs. 10~17, The reaction forces at impact point B and support point A increase with dynamic increasing loading rates irrespective of visco- plasticity plasticity of specimens. In particular, reaction forces and gap opening displacements at impacting point B and supporting point A for visco-plastic specimens tend to become higher than those of non-visco plastic specimens.

Figs. 18~21 show that maximum strain rates of non-visco plastic specimens increases with increasing loading rates. The strain rate reaches maximum values in shorter times as loading rates increase.

For visco-plastic specimens as shown in Figs. 2 3~26, maximum strain rates increase and occur later with loading rates increasing. In general, maximum strain rates for non-visco plastic specimens are much higher than those for visco-plastic specimens. This information on the tendering of strain rates is useful for predicting fracture time by dynamic crack.

From Figs. 27~28, we note that crack tip opening displacement(CTOD) increases with increasing loading rate irrespective of visco-plasticity of material. However, CTOD of a visco-plastic specimen becomes smaller than that of a non-visco plastic specimen. As is seen in Fig. 29, the viscoplasticity reduces the bouncing time of specimen(the time of gap opening displacement;no force growth) and increases the force growth rate when contact is established between the midsupport and the specimen.

6. Conclusions

The results of computer simulation analysis for the three point bend specimen of mild steel under various dynamic loading conditions are summarized as follows:

1) Reaction forces and gap opening displacement at impacting and supporting points of visco-plastic specimens are larger than those of non-visco plastic specimens.

2) The dynamic fracture of material is strongly influenced by the strain rate at the crack tip.

3) As loading rates increase, the maximum strain rates at the crack tips occur earlier for non-visco plastic specimens but occur later for visco-plastic specimens

4) The maximum strain rates and CTOD of visco-plastic specimens are rather smaller than those of non-visco plastic specimens. We can make use of these results in determining stability in dynamic fracture of material.

REFERENCES

1. J.F. Kalthoff, "On Some Current Problems in Experimental Fracture Dynamics," Workshop on Dynamic Fracture, W.G.Knauss,etc., pp.11-35, 1983.
2. M.F. Kanninen, et al., "Dynamic Crack Propagation under Impact Loading," Nonlinear and Dynamic Fracture Mechanics, ASME AMD 35, pp. 185-200, 1979.

3. A.J. Rosakis,et al., "Caustics by Reflection and their Application to ELastic-Plastic and Dynami Fracture Mechanics," SPIE Conference on Photomechanics and Speckle Metrology, San Diego, California, 1988.
4. H.G.van Elst, "Assessment of Dynamic Fracture Propagation Resistance at Instrumented High Velocity Gas-gun Impact Tests on SENB-Specimens," ICF 6 , Vol. 5 ,pp. 3089-3097.1984.
5. J.Ahmad, et al.," Elastic-plastic Finite Element Analysis of Dynamic Fracture," Eng. Frac. Mech., Vol.17, No. 3 , pp. 235-246,1983.
6. G.Wihlborg,"Design and Application of a Rig for High Energy Impact Tests ," IUTAm Symposium, Tokyo, Japan,1985.
7. ABAQUS Manual,Version 4.8, Hibbit, Karlsson and Sorensen, Ino.1989.
8. Ouk S. Lee, et al.,"Dynamic Crack Growth in 3PB Ductile Steel Specimen," Proceedings of Asian Pacific Conference for Fracture and Strength'96, pp.913-916, 1996.
9. A.Bergmark,et al.,"Dynamic Crack Propagation in 3PB Ductile Steel Specimens," Technical Report, LUTFD2,TFHF-3045,Lund,Sweden, 1991.
10. L.E.MaLvern,"The Propagation of Longitudinal Waves of Plastic Deformation in a Bar of Material Exhibiting a Strain- Rate Effect," J.AppL- Mech. , Vol. 18, pp. 203-208, 1951.
11. B.Brickstad,"A Viscoplastic Analysis of Rapid Crack Propagation Experiments in Steel," J.Mech. Phys. Solids, Vol.31, No 4, pp.307-332,1983.